Novel ”vibrating wire like” NEMS and MEMS structures for low temperature physics

Eddy Collin, J. Kofler, Jean-Savin Heron, Olivier Bourgeois, Yuriy M. Bunkov, Henri Godfrin

Journal of Low Temperature Physics manuscript No.
(will be inserted by the editor)

Novel ”vibrating wire like” NEMS and MEMS structures for low temperature physics

E. Collin · J. Kofler · J.-S. Heron · O. Bourgeois · Yu. M. Bunkov · H. Godfrin

15.06.2009

Keywords Micromechanics, nanomechanics, dissipation process, quantum fluid probes

Abstract Using microfabrication techniques, it has become possible to make mechanical devices with dimensions in the micro and even in the nano scale domain. Allied to low temperature techniques, these systems have opened a new path in physics with the ultimate goal of reaching *the quantum nature of a macroscopic mechanical degree of freedom*[1]. Within this field, materials research plays a significant role. It ranges from the fundamental nature of the dissipation mechanisms at the lowest temperatures, to the non-linear behavior of mechanical oscillators. We present experimental results on cantilever structures mimicking the well known ”vibrating wire” technique, which present many advantages as far as the mechanical studies are concerned: the measurement is phase-resolved, they can be magnetomotive *and* electrostatically driven, and support extremely large displacements. Moreover, these devices can be advantageously used to study quantum fluids, making the link with conventional low temperature physics.

PACS numbers: 62.20.Dc, 62.40.+i, 81.40.Jj, 47.45.-n, 47.45.Ab

1 Introduction

Vibrating wires are a very common tool used in low temperature physics. A small piece of (usually superconducting) wire is immersed in a (quantum) fluid. From the damping and the frequency shift of the transverse resonance one can deduce the viscosity of the fluid[2]. This technique is effectively used to measure the lowest temperatures ever achieved *directly inside* superfluid ^{3}He[3,4], and has been proposed to build ultra-sensitive low temperature astro-particle detectors[5]. The low temperature mechanics of these wires (in vaccum) has been extensively studied, especially with superconducting filaments[6].

It has been realized with the first 4 K measurements of the Grenoble group[7] that Silicon devices can replace advantageously this ”classical” technique. Indeed, Aluminum-coated

Institut Néel
CNRS et Université Joseph Fourier,
BP 166, 38042 Grenoble Cedex 9, France
E-mail: eddy.collin@grenoble.cnrs.fr

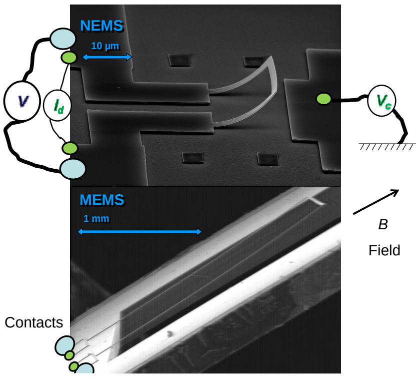

Fig. 1 (Color online) Two typical NbTi-coated structures mimicking the vibrating wire. Top: NEMS structure 200 nm thick, length 15 μm. The electrode on the right enables a capacitive coupling to the vibrating device. The metal layer is roughly 60 nm thick. Bottom: MEMS structure 5 μm thick, length 1.85 mm. The metal layer is roughly 150 nm thick. On both SEM pictures, one can see the curvature induced by the internal stress of the metallic layer created during the film growth[11]. This stress has an influence on the resonance position[12]. The drive and detection are also depicted, see text.

"goal-post" shaped MEMS[(1)] were tested in the range 1 K - 30 K, and they displayed perfeclty suitable characteristics[8]. Their dynamical parameters can be very well determined and fit to the 1D (linear *and* non-linear) oscillator.

Moreover, the "vibrating wire like" geometry is perfectly well suited for low temperature mechanics on its own[8]. The cantilever-based geometry enables to study fundamentals of mechanics at the lowest temperatures, and can be efficiently used especially to characterize mechanical properties of metallic coatings. In Fig. 1 we present two of these structures: one of the size of a conventianal vibrating wire (mm long, μm thick), and another one roughly 100 times smaller (μm long, nm thick) in the NEMS[(2)] domain. The actuation and detection scheme enables a phase resolved measurement (which is not the case of most optical techniques[9]), and the deflections supported by these structures can be huge (while they are limited for a doubly-clamped beam[10]).

2 Experimental details

The fabrication method of the MEMS device has been reported in[8,7]. It consists in a first chemical etching (KOH) releasing a thin membrane in a Si_3N_4 protected Silicon chip. The Nitride is then removed, and after a standard optical lithography we use Reactive Ion Etching to pattern the goal-post shape on it.

The NEMS device is obtained from SOI wafers[13]. After an e-beam lithography, the structure is patterned by means of Reactive Ion Etching. The 200 nm oxyde is then removed by a chemical vapour HF etching, releasing the device.

The excitation and detection scheme is the standard vibrating wire technique (see Fig. 1). A sinusoidal current $I_d \, cos(\omega t)$ is driven in the structure which lies in a static magnetic field B parallel to the chip surface. A magnetomotive force $I_d \, l \, B$ appears pulling the structure

[1] MEMS: micro-electro-mechanical-systems.
[2] NEMS: nano-electro-mechanical-systems.

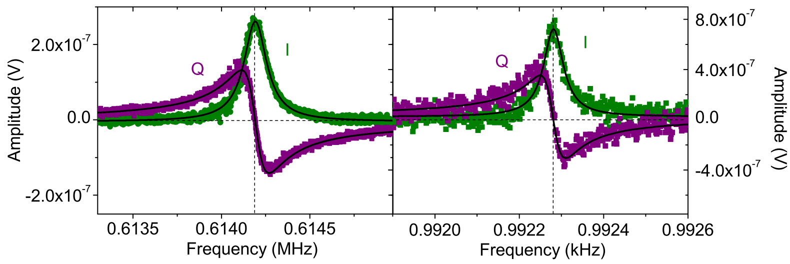

Fig. 2 (Color online) Linear resonance obtained for the transverse mode, at 4.2 K in vacuum. I and Q stand for phase and quadrature components respectively. Left: NEMS response with a current of 0.4 μA in a field of 540 mT. Right: MEMS response with a current of 0.3 μA in a field of 14 mT. The lines are Lorentzian fits.

out of the plane (l is the length of the pad). As the angular frequency ω is swept through the mode resonance ω_0 the structure starts to vibrate and an induced voltage $V = l B dx/dt$ appears at its ends (with x the top end displacement). It is detected with a lock-in amplifier giving acess to phase (I) and quadrature (Q). For the NEMS structure, a capacitor has been added to the design, enabling a voltage drive V_c.

Two typical resonance curves are shown in Fig. 2, in the superconducting state of the NbTi coating. The phase and quadrature components of the lines are perfectly Lorentzian, with a Q value of 4 000 for the NEMS and 17 000 for the MEMS respectively. While not particularly large, these values are within the literature [14,15]. Note that Aluminum coated vibrating wire MEMS [8] can reach Q values of the order of $0.5\,10^6$.

3 Results

Keeping the aspect ratios roughly constant, it is possible to compare directly the impact of the size (μm to nm) on the mechanical parameters: the internal friction mechanisms [16,17], the strength and elasticity of the metallic films deposited [18], the non-linear characteristics of the cantilevers and the superconducting-induced effects. In particular the damping mechanisms limiting the Q factors at low and ultra-low temperatures deserve to be understood [19,20]. In the present article, we shall discuss only a limited amount of points which we consider as most relevant. The whole of the experiment shall be published elsewere.

On Fig. 3 we show the characteristic displacement-force curve of the NEMS device, in the normal state. For the largest excitations, heating effects have been seen[(3)] and quantitatively measured ($\delta T < 2$ K for the 10 K data of Fig. 3). For our largest displacements, the NEMS structure started to behave non-linearly. The dynamic range explored is even wider than for our MEMS structures, but results are similar (Fig. 5 of ref. [8]).

The normal-state linear and non-linear behaviour of our MEMS structures is fairly well understood [8]. The non-linearity is of *geometrical* origin, leading to a frequency shift of the order or $\delta f = +0.1\, f_0\, x^2/h^2$ (h is the length of the cantilever). Thus the non-linearity is visible as soon as the shift is of the order of the linewidth Δf, which leads to the simple

[3] The line shifts and broadens, while keeping a Lorentz shape.

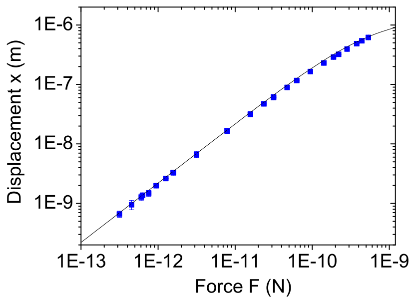

Fig. 3 (Color online) Displacement versus force curve for the NEMS structure, measured in vacuum at 10 K (normal state of the NbTi coating). The line is a fit enabling to "weigh" the device: we have typically $k \approx 1.5$ N/m (for the pair of cantilevers) and $m \approx 1.\,10^{-13}$ kg (for the vibrating mass). Note the dynamic range explored by the device. For an equivalent MEMS device, see Fig. 5 of ref.[8].

relation:

$$(x/h)^2 = 10/Q$$

from which we obtain numbers in the 10 μm - 20 μm range for x, that is of the order of 0.5 % to 1 % of h. When the non-linearity appears, the shape of the resonance becomes triangular with a frequency pulled upwards. At some critical excitation, the response gets bivalued[21].
In Fig. 3 the displacement of the end part of the NEMS reaches about 4 % of its length h, and indeed the line starts to become non-linear. However, the non-linearity is *very small and has the opposite sign* (it is pulled downwards), which deserves to be fully understood. In particular, the non-linear coefficient extracted from direct line fits is strain-dependent, and future experiments should clarify also its temperature dependence. It certainly is material-dependent (i.e. the NbTi layer) and perhaps linked to the huge distortion of the structure.
Moreover, a *measured linear regime extending over 2 orders of magnitude* is remarkable, and illustrates also the sensitivity of the setup. Indeed, the *linear dynamic range* is a figure of merit used in signal processing that can be applied to MEMS/NEMS in order to compare and characterize them[22].

On Fig. 4 we demonstrate the capacitive coupling to the device. To do so, we show our ability to tune the resonant frequency with an applied DC voltage V_c on the electrode. This voltage adds up a restoring force which in turn produces a restoring spring $\propto V_c^2$.

On Fig. 5 we illustrate the effects of superconductivity on the mechanical parameters (here, the frequency). Indeed, at low enough fields the frequency of the oscillator shifts up quadratically[23] with B. This effect had been reported already for our MEMS structure[24] down to 1 mT. It is easily understood as the 'pure' Meissner effect expelling the field lines from the superconductor, or an 'effective' Meissner effect obtained with strongly pinned vortices in the metal. In both cases the field lines distorsion gives rise to an additional spring constant (through the field lines energy gradient) leading to $f = \sqrt{f_0^2 + a\,B^2}$. The data are taken at low drives where the damping seems to be field and displacement independent. For stronger fields and drives, the frequency dependence is more complex, with additional dissipation occuring, certainly through vortex dynamics. The quadratic dependence factor a has been extracted and is plotted versus temperature in Fig. 5. It clearly reflects the supercon-

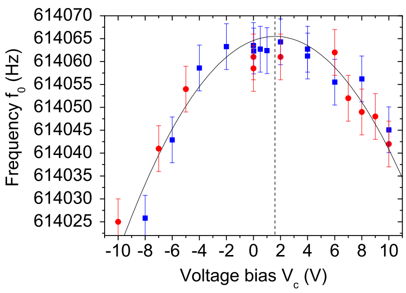

Fig. 4 (Color online) Tuning of the frequency by means of the capacitive coupling. A static voltage is applied V_c on the electrode while the resonance is swept with the standard technique. Data taken at 4.2 K (blue squares) and 10 K (red circles, shifted on the y axis), with low fields and small drives. The line is a quadratic fit, giving a coupling of -0.35 Hz/V^2.

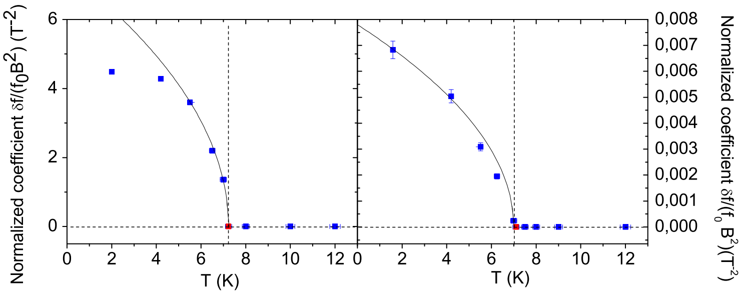

Fig. 5 (Color online) Quadratic factor extracted from the field induced frequency shift at small fields, as a function of temperature T. On the left: NEMS device. On the right: MEMS device. For both the NbTi T_c was about 7.3 K. The line is a $(T_c - T)^{0.5}$ guide (see text).

ducting transition with a power law dependance of $T_c - T$ close to T_c and a saturation at low temperatures. A fine understanding of the effect should lead to a quantitative analysis giving access, for instance, to the London penetration length $\lambda(T)$.

4 Conclusions

In this paper we presented new "vibrating wire like" MEMS and NEMS devices for low temperature studies. The mechanical resonance of these structures is obtained via the magnetomotive technique, furnishing a phase-resolved signal. The geometry allows for very strong displacements, and we can follow the vibration amplitude up to the non-linear regime of the MEMS and NEMS cantilevers.
Moreover, this technique is a convenient tool to study mechanics (for instance elasticity) of thin metallic films (both normal and superconducting), and could be used for viscometry in quantum fluids down to the 100 nm scale.

References

1. M. D. LaHaye, O. Buu, B. Camarota, K. C. Schwab, *Science* **304**, p. 74 (2004).
2. M.A. Black, H.E. Hall, K. Thomson, *Proc. 10th Int. Conf. on Low Temperature Physics*, p. 174 (1966); M.A. Black, H.E. Hall, K. Thomson, *J. Phys. C: Solid St. Phys.* **4**, p. 129 (1971).
3. A.M. Guénault, V. Keith, C.J. Kennedy, S.G. Mussett and G.R. Pickett, *J. of Low Temp. Phys.* **62**, p. 511 (1986).
4. C. Bäuerle, Yu.M. Bunkov, S.N. Fisher and H. Godfrin, *Phys. Rev. B* **57**, p. 14381 (1998); C.B. Winkelmann, E. Collin, Yu.M. Bunkov, H. Godfrin, *J. of Low Temp. Phys.* **135**, p. 3 (2004).
5. C.B. Winkelmann, J. Elbs, Yu.M. Bunkov, E. Collin, H. Godfrin, M. Krusius, *Nuclear Instr. and Methods in Physics Research* **A 574**, p. 264 (2007).
6. R. König, P. Esquinazi and F. Pobell, *J. of Low Temp. Phys.* **90**, p. 55 (1993).
7. S. Triqueneaux, E. Collin, D. J. Cousins, T. Fournier, C. Bäuerle, Yu. M. Bunkov and H. Godfrin, *Physica B* **284**, p. 2141 (2000).
8. E. Collin, Laure Filleau, Thierry Fournier, Yuriy M. Bunkov and Henri Godfrin, *J. of Low Temp. Phys.* **150**, no 5-6, p. 739 (2008).
9. Dustin W. Carr, S. Evoy, L. Sekaric, H. G. Craighead, and J. M. Parpia, *Appl. Phys. Lett.* **75**, p. 920 (1999).
10. Guiti Zolfagharkhani, Alexei Gaidarzhy, Seung-Bo Shim, Robert L. Badzey, and Pritiraj Mohanty, *Phys. Rev. B* **72**, 224101 (2005).
11. Michel Godin, Vincent Tabard-Cossa, and Peter Grütter, Peter Williams, *Appl. Phys. Lett.* **79**, p. 551 (2001).
12. Andrew W. McFarland, Mark A. Poggi, Margaret J. Doyle, and Lawrence A. Bottomley, Jonathan S. Colton, *Appl. Phys. Lett.* **87**, 053505 (2005).
13. J.-S. Heron, T. Fournier, N. Mingo and O. Bourgeois, *Nano Letters* **9**, 1861 (2009).
14. R. E. Mihailovich and J. M. Parpia, *Phys. Rev. Lett.* **68**, p. 3052 (1992).
15. P. Mohanty, D.A. Harrington, K.L. Ekinci, Y.T. Yang, M.J. Murphy, and M.L. Roukes, *Phys. Rev. B* **66**, 085416 (2002).
16. C. Seoánez and F. Guinea, A. H. Castro Neto, *Phys. Rev. B* **77**, p. 125107 (2008).
17. R. Lifshitz and M. L. Roukes, *Phys. Rev. B* **61**, p. 5600 (2000).
18. M. A. Haque, and M. T. A. Saif, *PNAS* **101**, p. 6335 (2005).
19. A. D. Fefferman, R. O. Pohl, A. T. Zehnder, and J. M. Parpia, *Phys. Rev. Lett.* **100**, p. 195501 (2008).
20. J. Classen, T. Burkert, C. Enss, and S. Hunklinger, *Phys. Rev. Lett.* **84**, p. 2176 (2000).
21. L.D. Landau and E.M. Lifshitz, *Mechanics*, third ed. Elsevier Science Ltd. (1976).
22. K. L. Ekinci, M. L. Roukes, *Rev. of Sci. Instr.* **76**, 061101 (2005); H. W. Ch. Postma, I. Kozinsky, A. Husain, and M. L. Roukes, *Appl. Phys. Lett.* **86**, 223105 (2005).
23. J. Kober, A. Gupta, P. Esquinazi, H.F. Braun, *Phys. Rev. Lett.*, **66**, p. 2507 (1991).
24. Poster session, "Superconductor coated electro-mechanical systems for low and ultra-low temperature physics", E. Collin, Y. Bilbao-Zarraga, Yu. M. Bunkov, H. Godfrin, *ULT 2008 conference frontiers of low temperature physics*, Royal Holloway University of London, England, 14-17 August 2008.